



A novel quinoline derivative containing a phenanthroimidazole moiety: Synthesis, physical properties and light-emitting diodes application

Xiaona Shao^a, Wenzhu Liu^a, Ruike Guo^a, Junfeng Chen^a, Nonglin Zhou^{a,b,*}

^a College of Chemistry and Materials Engineering, Huaihua University, Huaihua, 418000, China

^b Huaihua University Hunan Engineering Laboratory for Preparation Technology of Polyvinyl Alcohol (PVA) Fiber Material, Hunan, Huaihua, 418000, China

ARTICLE INFO

Keywords:

Phenanthroimidazole
Quinoline
Deep-blue emitting material
OLED
Hybrid WLED

ABSTRACT

The deep-blue emitting material 2-(8-(benzyloxy)quinolin-2-yl)-1-phenyl-1*H*-phenanthro[9,10-*d*]imidazole (**QL-PPI**) which contains 8-(Benzyloxy)quinoline core and phenanthroimidazole moiety, has been designed and synthesized. The non-doped OLED using **QL-PPI** as the emitting layer shows emission at 455 nm, full width at half maximum of 100 nm, maximum brightness of 250 cd m⁻², maximum current efficiency of 0.47 cd A⁻¹, and Commission Internationale de L'Eclairage (CIE) coordinate of (0.20, 0.22). Furthermore, the **QL-PPI** with a slight mass concentration in the silica gel is coated on the near ultraviolet (NUV) chip (380 nm) to prepare the hybrid deep-blue LED device **HB1** with a *y* coordinate = 0.0541. The hybrid WLED device **HW1** based on **QL-PPI** mixed with green phosphor [(Ba, Sr)₂SiO₄: Eu²⁺] and red phosphor [(Sr, Ca)₂AlSiN₃: Eu²⁺] is prepared. The hybrid WLED exhibits luminance efficiency of 18.05 lm W⁻¹ (at 19.90 mA), Correlated Color Temperature (CCT) of 4580 K, Color Rendering Index (CRI) of 80, and CIE chromaticity coordinate of (0.3571, 0.3562). These results reveal that the **QL-PPI** can apply both in OLED and the hybrid LED simultaneously. The **QL-PPI** which used in the hybrid WLED has the potential to reduce reliance on rare-earth metals and improve the CRI of the hybrid WLED.

1. Introduction

Since the multilayered organic light emitting diode (OLED) was firstly reported by Tang and VanSlyke in 1987, the OLED has received extensive attention due to its features of solid-state lighting and flexible and transparent displays [1]. In recent years, aryl substituted benzimidazole (PI) has attracted great attention in OLED field because of its simple synthesis [2], excellent thermal properties [3], high photoluminescence quantum yields (PLQYs) [4], and bipolar properties [5]. There are many high performance of OLED applications based on PI derivatives [6–9], and some of them can be used in preparing deep-blue OLED with a *y* coordinate ≤ 0.064 [10]. Simultaneously, the quinoline derivatives and its complexes have been extensively exploited. Some of them are suitable to be used in different opto-electronic devices or potential application in OLED device due to their photoluminescent properties [1,11–14]. Inspired by these, it was deemed to be a potentially viable strategy to connect the PI unit to the quinoline skeleton with a view to obtaining a deep-blue/blue emitting material [15].

An organic emitting material can be coated on the blue InGaN light-emitting diode (LED) to construct organic/inorganic hybrid white LED (WLED) which can convert the part of blue light into yellow or red light

to realize white light emission [16]. This structure of the hybrid device can avoid of the reliance on rare earth metal materials because the phosphors were substituted by organic emitting materials [17]. Some organic/inorganic hybrid WLED devices can obtain high luminance efficiency. And the CIE chromaticity coordinate of the organic/inorganic hybrid WLED can approach to (0.33, 0.33) [18,19]. For instance, Cali et al., constructed the organic/inorganic hybrid WLED device by employing GaN/InGaN as the blue LED and using the organic yellow emitting material as the under-conversion material. The device exhibits luminance efficiency of 118 lm W⁻¹ [20]. Sivakumar Vaidyanathan's team synthesized six yellow-orange trianiline derivatives of D-A structure. The CIE chromaticity coordinate of the organic/inorganic hybrid white light LED device is (0.32, 0.33). The CIE chromaticity coordinate value is very close to the ideal white light (0.33, 0.33) [21]. Although achievements have been made, the color rendering index (CRI) values of these devices are not mentioned. This may be due to the lack of blue-green/green light components in the emission spectra of WLED devices using the complementary color mode (BO mode) resulting in a low CRI which only higher values are acceptable for illumination applications. It is worth mentioning that, K.W. Cheah prepared RGB (three primary colors) organic/inorganic hybrid WLED devices with CIE

* Corresponding author. College of Chemistry and Materials Engineering, Huaihua University, Huaihua, 418000, China.

E-mail address: znl4615@163.com (N. Zhou).

<https://doi.org/10.1016/j.dyepig.2021.109198>

Received 11 December 2020; Received in revised form 24 January 2021; Accepted 26 January 2021

Available online 30 January 2021

0143-7208/© 2021 Elsevier Ltd. All rights reserved.

chromaticity coordinate of (0.321, 0.365) by using $\text{SrAl}_2\text{O}_4:\text{Eu}^{2+}$ as green phosphor, $\text{Sr}_4\text{Al}_{14}\text{O}_{25}:\text{Eu}^{2+}$ as blue phosphor, and $\text{Eu}(\text{BTFa})_3\text{Phen}$ as organic red emitting material however, the CRI value of the device was not reported [22].

However, there are few reports concerning the deep-blue/blue emitting materials applied both in OLED and the organic/inorganic hybrid LED simultaneously. In this work, in order to achieve this target, the new organic deep-blue emitting material 2-(8-(benzyloxy)quinolin-2-yl)-1-phenyl-1*H*-phenanthro[9,10-*d*]imidazole (**QL-PPI**) was designed and synthesized. The thermal, photophysical properties and the light-emitting diodes application of the **QL-PPI** were investigated.

2. Experiment section

2.1. Materials

The main reagents are described here. Petroleum ether (PE), Ethyl acetate (EtOAc), 1,4-Dioxane, Selenium dioxide (SeO_2), Ammonium acetate, Tetrahydrofuran (THF), Acetonitrile (MeCN) and Dichloromethane (DME) were received from Shanghai Titan Scientific Co., Ltd. Benzyl chloride and 2-Methyl-8-quinolinol were acquired from Shanghai Energy Chemical. All materials were used without further purification unless otherwise stated. The green ($\text{BaSi}_2\text{N}_2\text{O}_2:\text{Eu}^{2+}$) and red ($\text{Sr}, \text{Ca})_2\text{AlSiN}_3:\text{Eu}^{2+}$ phosphors were purchased from Shenzhen looking long technology co., Ltd. The near ultraviolet (NUV) LED chips (380 nm) and organic silica gel were purchased from the same company.

2.2. General procedures

^1H and ^{13}C NMR spectra were obtained on a Bruker ACF400 (400 MHz) spectrometer in chloroform-*d* (CDCl_3) with tetramethylsilane as reference. Elemental analysis was performed on a VarioMICROCHNOS elemental analyzer. UV-Vis absorption and photoluminescence spectra of THF solution and film were collected with Thermo Evolution 300 UV-Vis spectrophotometer and Hitachi F-7000 fluorescence spectrophotometer, respectively. Differential scanning calorimeter (DSC) was undertaken using a TA Q20 instrument under nitrogen atmosphere at a heating rate of $10\text{ }^\circ\text{C min}^{-1}$. Thermo gravimetric analysis (TGA) was carried out on a TA Q500 thermo gravimetric analyzer under nitrogen atmosphere at a heating rate of $10\text{ }^\circ\text{C min}^{-1}$. Cyclic voltammetry (CV) was recorded on a CHI-600C electrochemical analyzer. The measurements were determined using a conventional three-electrode configuration consisting of a glassy carbon working electrode, a platinum-disk auxiliary electrode and an Ag/AgCl reference electrode. And the scan rate was 10 mV s^{-1} . DFT calculations were performed to characterize the 3D geometries and the frontier molecular orbital energy levels of **QL-PPI** at the B3LYP/6-31G(d) level by using the Gaussian 03 program. All measurements were conducted at room temperature.

2.3. Device fabrication and measurement

The OLED device was fabricated by vacuum thermal evaporation technology. Before the deposition of an organic layer, the indium tin oxide (ITO) substrate was rinsed in an ultrasonic bath by the following sequences: in acetone, methyl alcohol, distilled water and kept in isopropyl alcohol for 48 h and dried by N_2 gas gun. The clean substrate was treated with oxygen plasma under the conditions of 10^{-2} Pa at 80 W for 3 min. The deposition rate of organic compounds was $0.7\text{--}1.4\text{ \AA s}^{-1}$. Finally, a cathode composed of LiF (1 nm) and aluminum (100 nm) were sequentially deposited onto the substrate in the vacuum of 5×10^{-4} Pa. All of properties of the OLED device such as *J-V-B* curves, current efficiency (CE), and CIE chromaticity coordinates of devices were measured with a Keithley 2400 Source meter and Chroma meter CS-2000. The hybrid organic/inorganic blue LED device was prepared with a structure of "near ultraviolet LED chips + organic blue emitting materials". The organic/inorganic hybrid WLED device was fabricated with the similar

structure. The commercial ($\text{Ba}, \text{Sr})_2\text{SiO}_4:\text{Eu}^{2+}$ and ($\text{Sr}, \text{Ca})_2\text{AlSiN}_3:\text{Eu}^{2+}$ were used as the green and red phosphors, respectively. The green/red phosphors and organic blue emitting materials were weighted in a certain proportion (For example, the emitting material mass concentration of 0.4% in this work means that the compound weight is 0.4% of the total mass of silica gel, and the total weight of silica gel in each device involved in this work is 1.5 g), and then mixed with organic silica gel thoroughly. In this step, the organic silica gel was composed of A glue and B glue. A/B silica gel was mixed according to the weight ratio of 1 (0.3 g):4 (1.2 g). After stirring evenly, vacuum defoaming was conducted for 30 min. The NUV LED chips (380 nm) were coated by the mixture of organic silica gel to produce hybrid LED devices. After the mixture of organic silica gel being solidified at $120\text{ }^\circ\text{C}$ for 1.0 h, the obtained hybrid LED devices were used for the subsequent test. All properties of the hybrid LED devices such as spectra, luminance efficiency, CCT, CRI and CIE chromaticity coordinate of devices were measured with an Everfine WY power source and SC-CK-09 LED test system. All measurements were carried out at room temperature under ambient conditions.

2.4. Synthesis

The intermediate products and designed compound were synthesized as outlined in Scheme 1.

2.4.1. 8-(Benzyloxy)-2-methylquinoline (2)

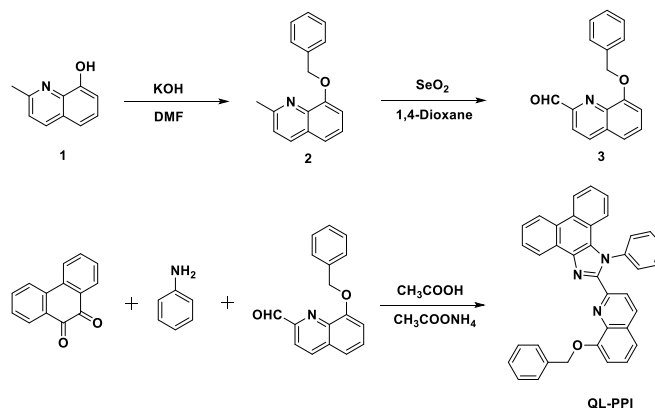
8-(Benzyloxy)-2-methylquinoline was prepared according to literature [23]. White solid.

2.4.2. 8-(Benzyloxy)quinoline-2-carbaldehyde (3)

8-Benzyloxy-2-methylquinoline (5.0 g, 20.06 mmol) and selenium oxide (2.67 g, 24.07 mmol) were added in 1,4-dioxane (400 mL) and the mixture was stirred under nitrogen at $105\text{ }^\circ\text{C}$ for 3 h. The 1,4-dioxane solvent was removed under reduced pressure, the crude product was purified by chromatography on a silica gel column (PE/EtOAc = 10/1 as eluent) to give the title compound 3.7 g (70.7%). ^1H NMR (400 MHz, CDCl_3) δ 10.34 (s, 1H), 8.28 (d, $J = 8.4$ Hz, 1H), 8.08 (d, $J = 8.4$ Hz, 1H), 7.56 (dd, $J = 12.8, 7.6$ Hz, 4H), 7.41 (ddd, $J = 20.4, 14.8, 7.7$ Hz, 7H), 7.17 (d, $J = 7.7$ Hz, 1H), 5.50 (s, 2H). ^{13}C NMR (101 MHz, CDCl_3) δ 193.98, 155.14, 151.55, 140.27, 137.29, 136.51, 131.43, 129.67, 128.72, 128.55, 128.04, 127.62, 127.10, 126.98, 119.94, 117.87, 110.97, 71.07. Found C, 77.70; H, 4.88; N, 5.23%; molecular formula $\text{C}_{17}\text{H}_{13}\text{NO}_2$; requires C, 77.55; H, 4.98; N, 5.32%.

2.4.3. 2-(8-(Benzyloxy)quinolin-2-yl)-1-phenyl-1*H*-phenanthro[9,10-*d*]imidazole (QL-PPI)

Compound **QL-PPI** was prepared according to the method reported in the literature [7,10]. 9,10-Phenanthrene-9,10-dione (0.42 g, 2.02 mmol),



Scheme 1. Synthetic routes and molecular structure of **QL-PPI**.

aniline (0.28 g, 3.03 mmol), 8-(benzyloxy)quinoline-2-carbaldehyde (0.53 g, 2.02 mmol), ammonium acetate (NH_4OAc , 1.09 g, 14.12 mmol), and acetic acid (HOAc , 10 mL) were added into flask, followed with refluxed for 12 h under argon (Ar) environment. The reaction solution was cooled down to room temperature, then deionized water was poured into flask, then filtered. The residue was purified by column chromatography on silica gel using ethyl PE/EtOAc at 10:1 by volume as the eluent to give a white powder with yield of 75.0% (0.80 g): ^1H NMR (400 MHz, CDCl_3) δ 8.94 (dd, $J = 8.4, 3.6$ Hz, 1H), 8.72 (dd, $J = 20.4, 8.3$ Hz, 2H), 8.54 (d, $J = 8.6$ Hz, 1H), 8.16 (d, $J = 8.6$ Hz, 1H), 7.82–7.72 (m, 1H), 7.70–7.58 (m, 3H), 7.53–7.44 (m, 1H), 7.45–7.15 (m, 11H), 7.07 (dd, $J = 8.3, 1.3$ Hz, 1H), 6.85 (dd, $J = 7.3, 1.6$ Hz, 1H), 5.21 (s, 2H). ^{13}C NMR (101 MHz, CDCl_3) δ 154.63, 149.48, 148.37, 139.75, 139.56, 137.56, 137.28, 136.20, 129.76, 129.54, 129.33, 129.23, 128.82, 128.74, 128.58, 128.52, 127.88, 127.36, 127.26, 127.05, 126.35, 125.78, 125.23, 124.05, 123.26, 123.20, 122.83, 122.52, 121.54, 119.57, 110.34, 70.28. Found C, 84.09; H, 4.56; N, 8.63%; molecular formula $\text{C}_{37}\text{H}_{25}\text{N}_3\text{O}$; requires C, 84.23; H, 4.78; N, 7.96%.

3. Result and discussion

3.1. Synthesis and thermal properties of QL-PPI

The synthesis of QL-PPI is outlined in Scheme 1, involving a series of hydroxyl protection reaction (benzylation), oxidation reaction and Debus-Radziszewski reaction (see Experiment section). As described in Fig. 1, the decomposition temperature (T_d , 5% weight loss) value of the compound QL-PPI was evaluated to be 407 °C. The DSC (Fig. 1 insert) analysis uncovered that the glass transition temperature (T_g) of QL-PPI was 92 °C. Moreover, no distinct crystalline peak was observed at a temperature beyond T_g . The small molecular compound QL-PPI has terrific thermodynamic stability due to molecular rigidity. The related data are listed in Table 1.

3.2. Optical properties and energy levels

The normalized UV–Vis absorption and photoluminescence (PL) spectra of QL-PPI in THF solution (1×10^{-5} M) and thin films (quartz plate) are shown in Fig. 2, relevant data are summarized in Table 1. In the THF solution, there are three peaks located at around 330–406 nm in the UV–Vis absorption spectra of QL-PPI. The absorption peak in the range of 345 nm can be assigned to the π - π^* transition of the substituent of 2-imidazole to the imidazole unit. A lower-energy band with peaks at around 365 and 380 nm can be assigned as the π - π^* transition and an

intramolecular charge transfer (ICT) band from the phenanthro[9,10-*d*]imidazole moiety to the 8-(benzyloxy)quinolin group [24]. The absorption bands are observed in the range of 300–325 nm approximately match to the quinoline group π - π^* transition [25]. Compare the UV–Vis absorption spectra of THF solution with that of thin films, the shape and peak position of QL-PPI are similar. No obvious red-shift of absorption peaks manifests that no crystallization occurs in the films [26,27]. Notably, as shown in Fig. 2, three peaks located at around 330–406 nm in absorption spectra are not obvious than that in thin films. The peak at about 380 nm was redshift to 390 nm and enhanced greatly. This is owing to the dispersed state of the QL-PPI in solution and the aggregation state of the QL-PPI in solid film [28]. In the aggregated state, there is a large molecular interaction between skeleton of the 8-(benzyloxy)quinolin group or the phenanthro[9,10-*d*]imidazole moiety, which changes the absorption peak intensity.

In the THF solution, the QL-PPI exhibits maximum PL (PL_{max}) value at deep-blue wavelengths of 421 nm. As shown in Fig. S3, its emission wavelength red-shifted (429 nm in MeCN solution) with increasing solvent polarity, implying the emission originating from the ICT state [29]. The photoluminescence quantum yields (PLQYs) of compound QL-PPI was tested by using *trans*-1-(9-anthryl)-2-phenylethene (*t*-APE, PLQYs 0.46 in MeCN) as the reference substance, the PLQYs of compound QL-PPI reached 0.77. The full width at half maximum (FWHM) of the deep-blue spectrum is 58 nm. Nevertheless, the maximum emission peak in PL spectrum of the QL-PPI in thin film state showed large red-shift about 34 nm with FWHM of 82 nm, comparing with its PL spectrum in THF solution. The red-shift of the emission observed in the film state is probably due to the presence of strong intermolecular interactions or aggregation in film states.

To obtain a good understanding on the optical properties in the molecular level, density functional theory (DFT) calculations (B3LYP/6-31G(d)) were carried out by using Gaussian 03 software [30]. The optimized geometry and the electron distribution of the compound QL-PPI are shown in Fig. 3. The calculation results indicate that the QL-PPI is not a planar molecule structure. There exists a dihedral angle of the QL-PPI between benzene ring and imidazole ring and dihedral angle between benzyloxy and quinoline ring. However, quinoline ring is coplanar with phenimidazole ring. The HOMO and LUMO orbitals of the QL-PPI are located on quinoline ring and phenimidazole ring. Thus, it is suggesting that the QL-PPI shows enhanced absorption peaks locating at 330–406 nm and more red-shifted emission in the film comparison to solution, which is consistent with our experimental results.

In order to measure the HOMO values of the compound QL-PPI, cyclic voltammetry (CV) measurements using a three-electrode cell were conducted (See ESI Fig. S4). The edge of the UV–Vis spectra was used to calculate the band gap (E_g) of the QL-PPI. The band gaps and the HOMO and LUMO levels are summarized in Table 1. The HOMO and LUMO level of the QL-PPI is -5.9 eV and -2.9 eV, respectively. This result implies that the QL-PPI is easy to inject an electron in the OLED.

3.3. Non-doped blue OLED

To investigate the potential application of the compound QL-PPI, non-doped OLED with the configuration of ITO/NPB (25 nm)/QL-PPI (40 nm)/TPBi (15 nm)/LiF (1 nm)/Al (100 nm) was fabricated. In this device, *N,N'*-Di-1-naphthyl-*N,N'*-diphenylbenzidine (NPB), QL-PPI, and 1,3,5-tris(1-phenyl-1*H*-benzimidazol-2-yl)benzene (TPBi) were acted as the hole-transport layer (HTL), emitting layer (EML) electron-transport layer (ETL), respectively [31]. LiF was employed as the electron-injecting layer (EIL) and Al metal served as the cathode [32]. The device configuration and the energy level diagrams of used materials are shown in Fig. 4.

The electroluminescence (EL) spectrum, current density-voltage-brightness (J - V - B) characteristics, CE, and PE of the non-doped OLED device using compound QL-PPI as the emitting materials are shown in

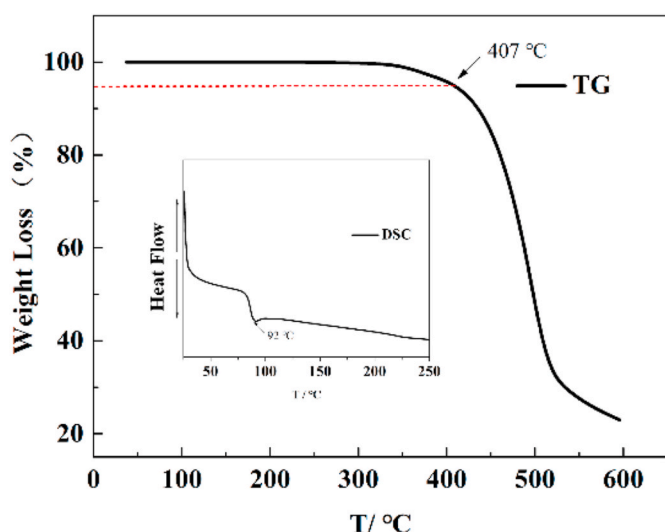


Fig. 1. TGA and DSC thermogram (insert) of QL-PPI.

Table 1

The optical, thermal properties and energy levels of the as-synthesized compound.

Compound	$T_d^{[a]}$ (°C)	$T_g^{[b]}$ (°C)	$\lambda_{abs}^{[c]}$ (nm)	PL ^[d] (nm)	$E_g^{[e]}$ (eV)	HOMO ^[f] (eV)	LUMO ^[g] (eV)	$\Phi_r^{[h]}/\Delta\lambda^{[k]}$ (nm)
QL-PPI	407	92	300,345,365,380 /300,350,375,390 ^[h]	421/455 ^[h]	3.0	-5.9	-2.9	0.77/56

[a] Measured by TGA at a heating rate of $10\text{ }^\circ\text{C min}^{-1}$ under nitrogen atmosphere. [b] Measured by DSC according to the heat-cool-heat procedure. [c] Absorption spectra were recorded in the $1.0 \times 10^{-5}\text{ mol L}^{-1}$ THF solution. [d] PL spectra were recorded in the $(1.0 \times 10^{-5}\text{ mol L}^{-1})$ THF solution. [e] Optical energy gaps calculated from the absorption threshold from UV-Vis absorption spectrum of THF solution. [f] Measured with CV. [g] $|\text{LUMO}| = |\text{HOMO}| - E_g$. [h] Absorption or PL peaks of thin films. [i] PLQYs of compound QL-PPI (relative value). [k] Stokes shift of compound QL-PPI (in THF solution).

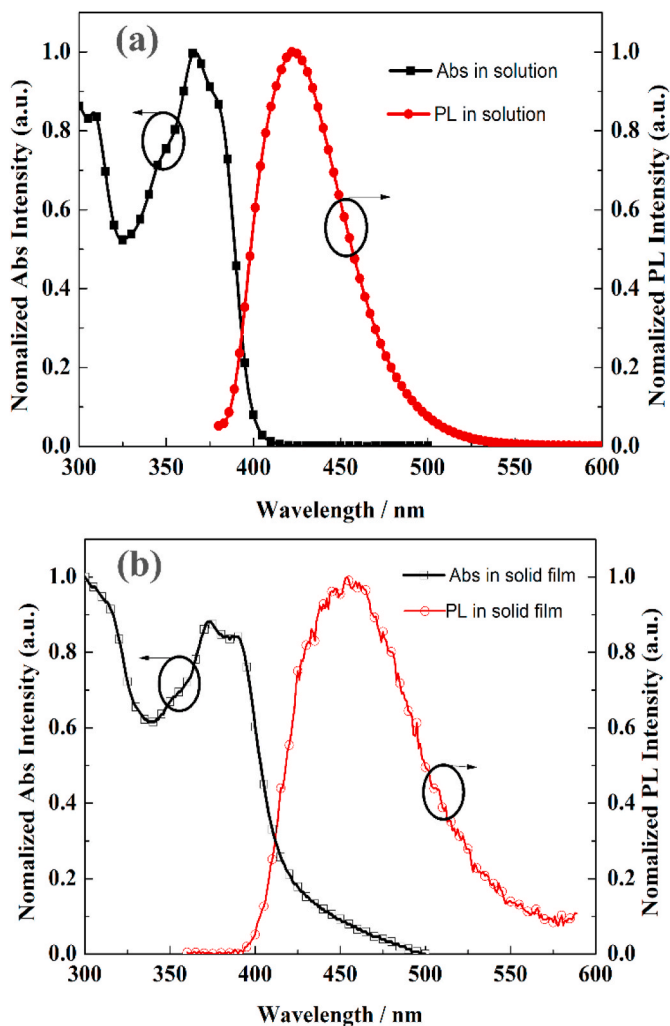


Fig. 2. UV-Vis absorption and PL spectra of QL-PPI (a) dilute solution ($1 \times 10^{-5}\text{ M}$) in THF and (b) neat thin films.

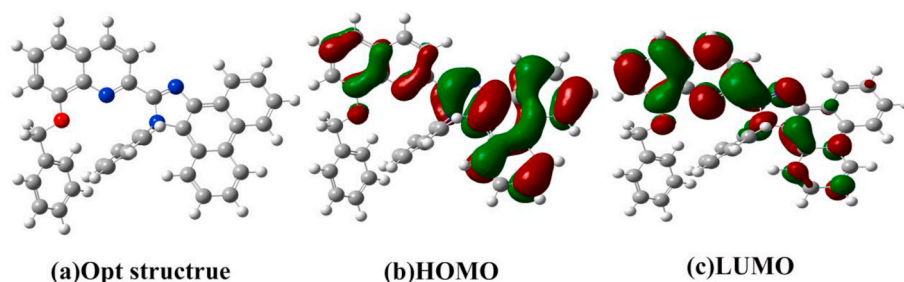


Fig. 3. Molecular structures (a) and electron density distributions of the HOMO (b)/LUMO (c) calculated with B3LYB/6-31G(d).

Fig. 5. All the device data are listed in Table 2. As can be seen in Fig. 5a, the device shows a main peak centered at the 455 nm with FWHM 100 nm. The corresponding CIE coordinate of the OLED device is (0.20, 0.22) which located at sky blue region. The main peak of the EL spectrum of the OLED device is coincident with the film PL spectrum of compound QL-PPI. However, there is shoulder peak generated at the 600 nm making the FWHM of spectrum expanded to 100 nm. As can be seen from Fig. 4a, the HOMO and LUMO level of QL-PPI is -5.9 eV and -2.9 eV , respectively. This implies that the QL-PPI is easy to inject an electron and hard to inject hole from NPB to QL-PPI in the OLED, due to the large energy barrier between NPB and QL-PPI and narrow energy barrier between TPBi and QL-PPI. Then we suggest the shoulder peak at 600 nm in spectrum of OLED device comes from electrophilic that originates from the direct optical transition across QL-PPI and NPB interface, which result in the FWHM of spectrum expanded to 100 nm [33]. The non-doped OLED device exhibits a maximum brightness of 250 cd m^{-2} , turn-on voltage (defined as the operation voltage at brightness of 1 cd

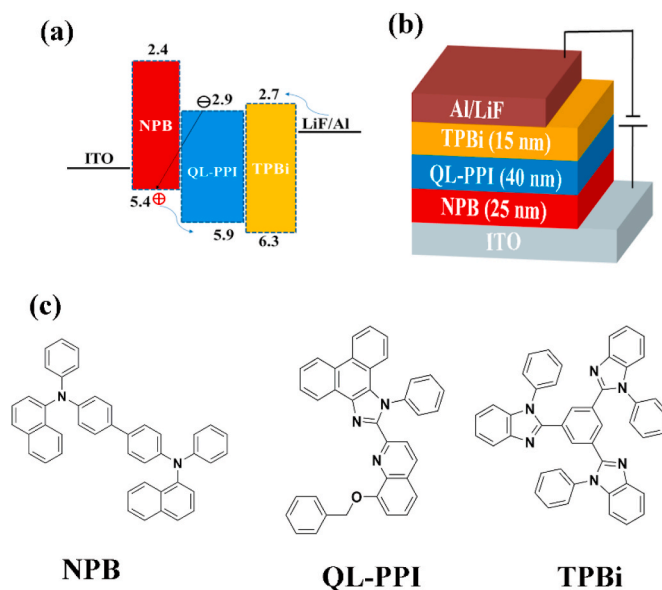


Fig. 4. The device energy-level diagram (a), configuration (b) and molecular structures of the materials used in this study (c).

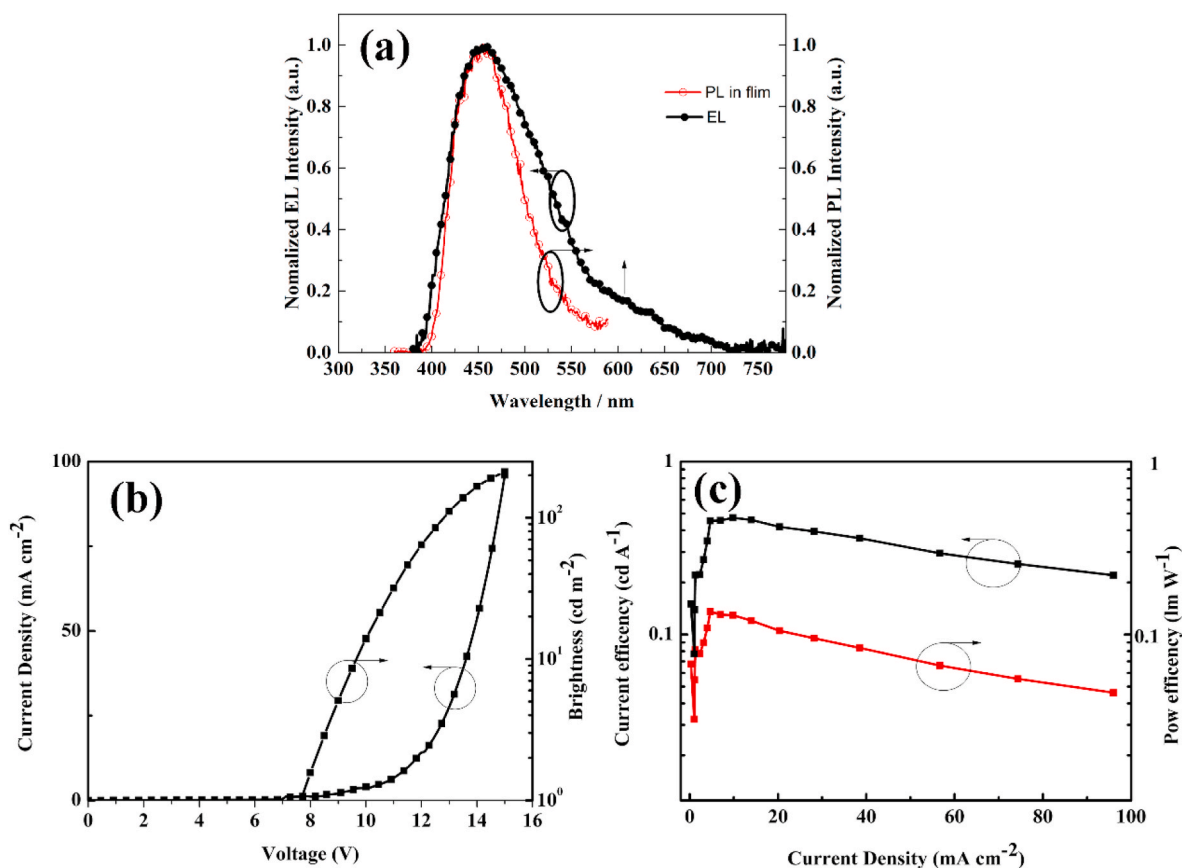


Fig. 5. (a) Electroluminescence spectra of devices. (b) current density-voltage-brightness (J - V - B) characteristics. (c) current efficiencies and power efficiencies versus current density.

Table 2

Key performance parameters of the Non-doped blue OLED.

Compound	Turn-on Voltage ^a /V	Brightness (cd m ⁻²)	CE ^b (cd A ⁻¹)	PE ^c (lm W ⁻¹)	EL ^d _{λmax} /nm	FWHM/nm	CIE ^d 1931 (x,y)
QL-PPI	8	250	0.47	0.14	455	100	0.20,0.22

^a Recorded at 1 cd m⁻².

^b Max Current efficiency.

^c Max Power efficiency.

^d Recorded at 10V.

m⁻²) of 8 V, maximum CE of 0.47 cd A⁻¹, maximum PE of 0.14 lm W⁻¹. Though the device manifests not overly impressive performance, we believe the device performance can be further improved by changing different holes transport functional layer which can match the energy level with the QL-PPI.

3.4. Hybrid deep-blue LED and WLED

As the QL-PPI shows deep-blue emission in the THF solution, the QL-PPI with a mass concentration of 0.4% in the silica gel is coated on the NUV chip (380 nm) to prepare the hybrid deep-blue LED device (HB1). The device data are listed in Table 3. The EL spectrum and CIE chromaticity coordinate of device HB1 are shown in Fig. 6ab. The peak value of the emission spectrum of device HB1 is located at 421 nm which is consistent with the spectrum in THF solution. The device HB1 exhibits deep-blue emission with CIE chromaticity coordinate of (0.1620, 0.0541). Moreover, device HB1 demonstrates performance with luminance efficiency of 2.94 lm W⁻¹ at 19.90 mA which is much better than that of OLED device. It can be inferred that the concentration of QL-PPI

Table 3

Key performance parameters of the hybrid deep-blue LED and WLED.

Device	Current (mA)	CCT (K)	CRI	CIE 1931 (x, y)	Luminance Efficiency (lm W ⁻¹)
HB1	19.90	–	–	0.1620, 0.0541	2.94
HW1	19.90	4580	80	0.3571, 0.3562	18.05

in silica gel is low, which can effectively inhibit its fluorescence quenching in device.

In order to further expand the application of the QL-PPI in organic/inorganic hybrid WLED devices, the inorganic WLED devices were fabricated firstly. The inorganic WLED devices were constructed by using the blue (BaMgAl₁₀O₁₇: Eu²⁺), green (Ba, Sr)₂SiO₄: Eu²⁺ and red (Sr, Ca)₂AlSiN₃: Eu²⁺ phosphors. In order to obtain the equivalent spectral intensity of blue, green and red light in the EL spectra of

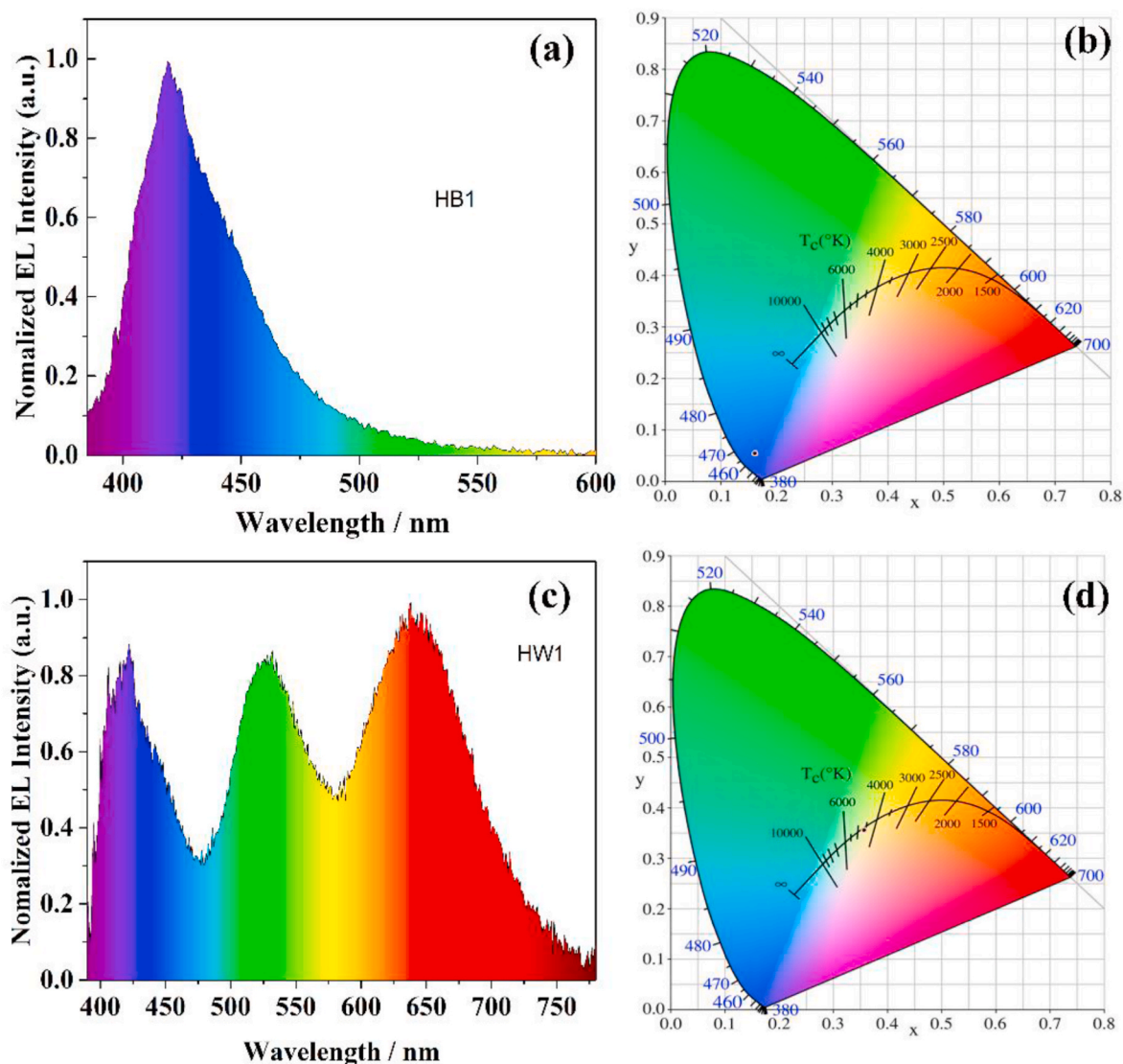


Fig. 6. (a) the EL spectrum and CIE chromaticity coordinate (b) of the device HB1. (c) the EL spectrum and CIE chromaticity coordinate (d) of the device HW1.

inorganic WLED devices (so that the CIE coordinates of the devices are close to the ideal white light), we first studied the concentration formula of the tri-phosphor in the devices. Considering the blue light that emitting from blue phosphors can be absorbed by green and red phosphors [34,35], the WLED devices should be appropriate increase in the concentration of the blue phosphors. In order to further verify the correctness of this conjecture, the concentration of green phosphor (3.2%) and red phosphor (2.6%) are kept unchanged except the concentration of blue phosphor was changed. The WLED devices properties are summarized in Table S1. As shown in Figure. S5, when the concentration of blue phosphor increases from 1.2% to 4% (devices W1, 2, 3, 4), the intensity of blue light in the EL spectra of inorganic WLED devices is very weak. The CIE coordinates of the four devices indicate that the WLED devices emit warm white light although the CRI of the four WLED devices can reach 83. This phenomenon is terminated in device W5 which the concentration of blue phosphor is 14%. The emission intensity of blue light is improved obviously in the device W5. The CIE coordinate and CRI of the device W5 are (0.3941, 0.3774), 74.4, respectively. However, the concentration of blue phosphor is high in the device W5 increasing an urgent need to reduce blue phosphor or replace blue phosphor with organic blue emitting materials to reduce reliance on rare-earth metals.

Inspired by these well-founded facts, we believe using the QL-PPI as

deep-blue emitting material to replace the blue phosphor to construct hybrid WLED device can reduce the reliance on rare earth metals. The WLED device HW1 based on the QL-PPI mixed with green phosphor $[(\text{Ba}, \text{Sr})_2\text{SiO}_4: \text{Eu}^{2+}]$ and red phosphor $[(\text{Sr}, \text{Ca})_2\text{AlSiN}_3: \text{Eu}^{2+}]$ is prepared. In device HW1, the silica gel total mass concentration of the QL-PPI, green phosphor and red phosphor are 0.4%, 3.2% and 2.6%, respectively. The EL spectrum and CIE chromaticity coordinate of device HW1 are illustrated in Fig. 6cd. The device data are listed in Table 3. The deep-blue region is very strong in the EL spectrum. The device HW1 exhibits luminance efficiency of 18.05 lm W^{-1} (at 19.90 mA), CCT of 4580 K, CRI of 80, and CIE chromaticity coordinate of (0.3571, 0.3562). The CIE coordinate of device HW1 is very close to the ideal values of white light and the CRI value of 80 is much better than that of inorganic WLED device W5 which is 74.4.

4. Conclusion

In summary, the new deep-blue material, QL-PPI with 8-(benzyloxy) quinoline containing PI moiety, was designed and synthesized. The QL-PPI benefit from quinoline and PI skeleton, shows high thermal stability. The QL-PPI was employed as emitter to fabricate non-doped OLED. The OLED shows sky-blue emission due to the aggregation in the film and electroplex that originates from the direct optical transition across QL-

PPI and NPB interface. When using QL-PPI to construct a hybrid LED, the LED exhibits deep-blue emission with CIE chromaticity coordinate of (0.1620, 0.0541). In addition, the hybrid WLED device HW1 based on QL-PPI slightly mixed with green phosphor [(Ba, Sr)₂SiO₄: Eu²⁺] and red phosphor [(Sr, Ca)₂AlSiN₃: Eu²⁺] is prepared. The hybrid WLED shows better performance than that inorganic WLED (W5). The research work presented here provides a new emitting material to fabricate OLED and hybrid LED devices simultaneously. Further optimizing the hybrid WLED fabrication (improving the performance) and synthesizing quinoline complexes (based on QL-PPI) are currently in progress in our laboratory.

Author statement

Xiaona Shao: Participation in the whole work; drafting of the article; data analysis. Wenzhu Liu: Verification. Data curation. Ruike Guo: Prepare the hybrid LED devices, Investigation. Junfeng Chen: Synthesize the compounds of 8-(benzyloxy)-2-methylquinoline and 2-(8-(benzyloxy)quinolin-2-yl)-1-phenyl-1*H*-phenanthro[9,10-*d*]imidazole (QL-PPI). Nonglin Zhou: perception and design; prepared OLED; final approval of the version to be published.

Declaration of competing interest

The authors declare that they have no known competing financial interests or personal relationships that could have appeared to influence the work reported in this paper.

Acknowledgements

This work was supported by the Natural Science Foundation of Hunan Province, China (2020JJ5449), Scientific Research Fund of Hunan Provincial Education Department (20C1474), Scientific Research Program of Huaihua University (HHUY2018-06) and the Foundation of Hunan Double First-rate Discipline Construction Projects (HHUY2019-05). The calculation in this work was supported by high performance computing center of Tianjin University, China. The OLED device in this work was constructed in school of chemical engineering and technology, Tianjin University, China.

Appendix A. Supplementary data

Supplementary data to this article can be found online at <https://doi.org/10.1016/j.dyepig.2021.109198>.

References

- Tang CW, VanSlyke SA. Organic electroluminescent diodes. *Appl Phys Lett* 1987;51(12):913–5.
- Yuan Y, Li D, Zhang X, Zhao X, Liu Y, Zhang J, et al. Phenanthroimidazole-derivative semiconductors as functional layer in high performance OLEDs. *New J Chem* 2011;35(7):1534–40.
- Huang H, Wang Y, Wang B, Zhuang S, Pan B, Yang X, et al. Controllably tunable phenanthroimidazole-carbazole hybrid bipolar host materials for efficient green electrophosphorescent devices. *J Mater Chem C* 2013;1(37):5899–908.
- Ivanauskaitė A, Lygaitis R, Raisys S, Kazlauskas K, Kreiza G, Volyniuk D, et al. Structure-property relationship of blue solid state emissive phenanthroimidazole derivatives. *Phys Chem Chem Phys* 2017;19(25):16737–48.
- Huang H, Wang Y, Zhuang S, Yang X, Wang L, Yang C. Simple phenanthroimidazole/carbazole hybrid bipolar host materials for highly efficient green and yellow phosphorescent organic light-emitting diodes. *J Phys Chem C* 2012;116(36):19458–66.
- Gao Z-J, Yeh T-H, Xu J-J, Lee C-C, Chowdhury A, Wang B-C, et al. Carbazole/Benzimidazole-based bipolar molecules as the hosts for phosphorescent and thermally activated delayed fluorescence emitters for efficient OLEDs. *ACS Omega* 2020;5(18):10553–61.
- Zhou NL, Wang SR, Xiao Y, Li XG. A Novel trans-1-(9-Anthryl)-2-phenylethene derivative containing a phenanthroimidazole unit for application in organic light-emitting diodes. *Chem Asian J* 2018;13(1):81–8.
- Song Y-L, Jiao B-J, Liu C-M, Peng X-L, Wang M-M, Yang Y, et al. Synthesis, structures and luminescent properties of red emissive neutral copper(I) complexes with bisphosphino-substituted benzimidazole. *Inorg Chem Commun* 2020;112:107689.
- Zhang R, Sun H, Zhao Y, Tang X, Ni Z. Dipolar 1,3,6,8-tetrasubstituted pyrene-based blue emitters containing electro-transporting benzimidazole moieties: Syntheses, structures, optical properties, electrochemistry and electroluminescence. *Dyes Pigments* 2018;152:1–13.
- Fan S, You J, Miao Y, Wang H, Bai Q, Liu X, et al. A bipolar emitting material for high efficient non-doped fluorescent organic light-emitting diode approaching standard deep blue. *Dyes Pigments* 2016;129:34–42.
- Wei H, Yu G, Zhao Z, Liu Z, Bian Z, Huang C. Constructing lanthanide [Nd(III), Er(III) and Yb(III)] complexes using a tridentate N,N,O-ligand for near-infrared organic light-emitting diodes. *Dalton Trans* 2013;42(24):8951–60.
- Mishra A, Nayak PK, Periasamy N. Synthesis of 5-alkoxymethyl- and 5-amino-methyl-substituted 8-hydroxyquinoline derivatives and their luminescent Al(III) complexes for OLED applications. *Tetrahedron Lett* 2004;45(33):6265–8.
- Moon J, Lee J, Kim KJ, Lee H, Kim YK, Yoon SS. Blue fluorescent organic light-emitting diodes using 11,11-dimethyl-3-(10-phenylanthracen-9-yl)-11*H*-indeno [1,2-*b*]quinoline derivatives. *J Nanosci Nanotechnol* 2020;20(8):4652–6.
- Szlachcic P, Uchacz T. Influence of fluorine on the photophysical, electrochemical properties and basicity of 1,3-diphenylpyrazolo[3,4-*b*]quinoline derivatives. *J Lumin* 2018;194:579–87.
- Tao YT, Balasubramanian E, Danel A, Jarosz B, Tomasik P. Organic light-emitting diodes based on variously substituted pyrazoloquinolines as emitting material. *Chem Mater* 2001;13(4):1207–12.
- Smith R, Liu B, Bai J, Wang T. Hybrid III-nitride/organic semiconductor nanostructure with high efficiency nonradiative energy transfer for white light emitters. *Nano Lett* 2013;13(7):3042–7.
- Yue Z, Cheung YF, Choi HW, Zhao Z, Tang BZ, Wong KS. Hybrid GaN/Organic white light emitters with aggregation induced emission organic molecule. *Opt Mater Express* 2013;3(11):1906.
- Zhang L, Li B, Lei B, Hong Z, Li W. A triphenylamine derivative as an efficient organic light color-conversion material for white LEDs. *J Lumin* 2008;128(1):67–73.
- Findlay NJ, Bruckbauer J, Inigo AR, Breig B, Arumugam S, Wallis DJ, et al. An organic down-converting material for white-light emission from hybrid LEDs. *Adv Mater* 2014;26(43):7290–4.
- Caruso F, Mosca M, Macaluso R, Feltin E, Cali C. Generation of white LED light by frequency downconversion using perylene-based dye. *Electron Lett* 2012;48(22):1417.
- Kajjam AB, Kumar PSV, Subramanian V, Vaidyanathan S. Triphenylamine based yellowish-orange light emitting organic dyes (donor-π-acceptor) for hybrid WLEDs and OLEDs: synthesis, characterization and theoretical study. *Phys Chem Chem Phys* 2018;20(6):4490–501.
- Lee KM, Cheah KW, An BL, Gong ML, Liu YL. Emission characteristics of inorganic/organic hybrid white-light phosphor. *Appl Phys A Mater* 2005;80(2):337–9.
- Maffeo D, Williams JAG. Intramolecular sensitisation of europium(III) luminescence by 8-benzyloxyquinoline in aqueous solution. *Inorg Chim Acta* 2003;355:127–36.
- Zhang LK, Tong QX, Shi LJ. A highly selective ratiometric fluorescent chemosensor for Cd²⁺ ions. *Dalton Trans* 2013;42(24):8567–70.
- Santos FA, Tondato WN, Tame Parreira RL, Orenha RP, Leite Lourenço LC, da Silva de Laurentiz R. Synthesis and luminescent properties of new naphthoquinoline lactone derivatives. *J Lumin* 2020;227:117547.
- Wu C-S, Fang S-W, Chen Y. Solution-processable hole-transporting material containing fluorenyl core and triple-carbazolyl terminals: synthesis and application to enhancement of electroluminescence. *Phys Chem Chem Phys* 2013;15(36):15121–7.
- Liu Y, Xie C, Tan W, Liu X, Yuan Y, Xie Q, et al. Analysis of light-induced degradation in inverted perovskite solar cells under short-circuited conditions. *Org Electron* 2019;71:123–30.
- Sayin S, Varol SF, Merdan Z, Eymur S. Synthesis of isoniazid substituted pyrene (PINHy), and investigation of its optical and electrochemical features as tunable/flexible OLEDs. *J Mater Sci Mater Electron* 2017;28(17):13094–100.
- Zhang Y, Lai S-L, Tong Q-X, Lo M-F, Ng T-W, Chan M-Y, et al. High efficiency nondoped deep-blue organic light emitting devices based on imidazole-π-triphenylamine derivatives. *Chem Mater* 2011;24(1):61–70.
- Foresman JB, Head-Gordon M, Pople JA, Frisch MJ. Toward a systematic molecular orbital theory for excited states. *J Phys Chem* 1992;96(1):135–49.
- Li L, Liu X, Lyu L, Wu R, Liu P, Zhang Y, et al. Modification of Ultrathin NPB interlayer on the electronic structures of the CH₃NH₃PbI₃/NPB/MoO₃ interface. *J Phys Chem C* 2016;120(32):17863–71.
- Zhou N, Wang S, Xiao Y, Li X. Double light-emitting layer implementing three-color emission: using DCJTb lightly doping in Alq₃ as red-green emitting layer and APEAn1N as blue-green emitting layer. *J Lumin* 2018;196:40–9.
- Wang Y-M, Teng F, Xu Z, Hou Y-B, Yang S-Y, Qian L, et al. White emission via electroluminescence formation at poly(*N*-vinylcarbazole)/2,9-dimethyl-4,7-diphenyl-1,10-phenanthroline interface. *Appl Surf Sci* 2004;236(1–4):251–5.
- Shao Q, Lin H, Dong Y, Jiang J. Temperature-dependent photoluminescence properties of (Ba,Sr)₂SiO₄:Eu²⁺ phosphors for white LEDs applications. *J Lumin* 2014;151:165–9.
- Liu X, Song Z, Wang S, Liu Q. The red persistent luminescence of (Sr,Ca)AlSiN₃:Eu²⁺ and mechanism different to SrAl₂O₄:Eu²⁺, Dy³⁺. *J Lumin* 2019;208:313–21.